AGU PUBLICATIONS

Water Resources Research

RESEARCH ARTICLE
10.1002/2015WR017081

The effect of lateral confinement on gravel bed river morphology

G. A. Garcia Lugo[1,2], W. Bertoldi[2], A. J. Henshaw[1], and A. M. Gurnell[1]

[1]School of Geography, Queen Mary, University of London, London, UK, [2]Department of Civil, Environmental and Mechanical Engineering, University of Trento, Trento, Italy

Key Points:
- Lateral river channel confinement affects bed form and sediment transport
- Bed form is better characterized using new indices
- There is a smooth transition in bed form across river planform styles

Correspondence to:
W. Bertoldi,
walter.bertoldi@unitn.it

Citation:
Garcia Lugo, G. A., W. Bertoldi, A. J. Henshaw, and A. M. Gurnell (2015), The effect of lateral confinement on gravel bed river morphology, *Water Resour. Res.*, *51*, doi:10.1002/2015WR017081.

Received 9 FEB 2015
Accepted 30 JUL 2015
Accepted article online 4 AUG 2015

Abstract In this paper, we use a physical modeling approach to explore the effect of lateral confinement on gravel bed river planform style, bed morphology, and sediment transport processes. A set of 27 runs was performed in a large flume (25 m long, 2.9 m wide), with constant longitudinal slope (0.01) and uniform grain size (1 mm), changing the water discharge (1.5–2.5 L/s) and the channel width (0.15–1.5 m) to model a wide range of channel configurations, from narrow, straight, embanked channels to wide braided networks. The outcomes of each run were characterized by a detailed digital elevation model describing channel morphology, a map of dry areas and areas actively transporting sediment within the channel, and continuous monitoring of the amount of sediment transported through the flume outlet. Analysis reveals strong relationships between unit stream power and parameters describing the channel morphology. In particular, a smooth transition is observed between narrow channels with an almost rectangular cross-section profile (with sediment transport occurring across the entire channel width) and complex braided networks where only a limited proportion (30%) of the bed is active. This transition is captured by descriptors of the bed elevation frequency distribution, e.g., standard deviation, skewness, and kurtosis. These summary statistics represent potentially useful indicators of bed morphology that are compared with other commonly used summary indicators such as the braiding index and the type and number of bars.

1. Introduction

Although design strategies adopted in river restoration and flood protection increasingly reflect the view that an increase in river width is needed to improve bed morphological complexity and ecological quality [e.g., *Rohde et al*., 2004, 2005; *Jähnig et al*., 2009; *Weber et al*., 2009], few studies provide detailed quantitative information on the effect of different width constraints on river bed topography.

Fluvial geomorphologists have long explored the relationship between river planform style and external controlling parameters and this topic continues to be debated [*Leopold and Wolman*, 1957; *van den Berg*, 1995; *Eaton et al*., 2010; *Kleinhans and van den Berg*, 2011]. However, the focus of this mainly empirical, field-based, research is usually the natural state of a river rather than its state when constrained by embankments, other engineering structures, or by natural inerodible valley walls [*Fotherby*, 2009]. Other studies have considered the effect of different widths on alternate and multiple bar formation [*Fujita*, 1989] or on braided river sediment transport [*Marti and Bezzola*, 2006], but a detailed investigation on the morphological changes induced by lateral confinement is lacking.

A different and complementary line of research has been to explore the conditions that determine the formation of alternate, central, or multiple bars, which ultimately determine the river planform style, through an analytical investigation of the intrinsic instability of the river bed [e.g., *Parker*, 1976; *Colombini et al*., 1987; and recently *Crosato and Mosselman*, 2009]. Such theoretical frameworks generally require several simplifying hypotheses that are difficult to meet when the river configuration becomes more complex and a multichannel pattern emerges. For example, the transverse variability in flow, shear stress, and sediment transport in multichannel rivers makes the use of cross-section averaged parameters difficult [*Paola*, 1996; *Ferguson*, 2003]. The occurrence of wetted areas (or even dry areas) where sediment is not transported hinders or even prevents the use of most bar theories to explore the planform and bed configuration (but see *Seminara and Solari* [1998] for the possibility to extend analytical theories to partially transporting channel bends). Laboratory experiment [e.g., *Fujita*, 1989] and numerical model results [e.g., *McArdell and Faeh*,

2001] have demonstrated that bed topography in large channels evolves from multiple bars to central or alternate bars, with a reduction in bar mode through time that is not captured by theoretical models.

Last, the transition from a single thread to a braided pattern, and thus a transition from relatively simple and narrow to wider more complex bed configurations, has been generally described in terms of an increase in the braiding index (the number of anabranches per cross section) [*Egozi and Ashmore*, 2008]. However, this index is strongly dependent on flow stage [*van der Nat et al*., 2002; *Welber et al*., 2012] and attempts to establish a relationship with controlling parameters (bankfull discharge, grain size, and slope) have generally failed.

The increased availability of high-resolution digital elevation models (DEMs) provides opportunities for a more detailed characterization of river bed topography, and thus for a more detailed investigation of how more traditional measures of river width, the number and types of bars, planform style, and indices of planform complexity express true differences in river bed morphology. The development of topographical indices from this detailed three-dimensional information is crucial to better understand and characterize the relevant morphological processes controlling river adjustment. Such research is most effectively conducted in a laboratory flume, where responses to form and process manipulations can be investigated under controlled conditions. Moreover, as *Doeschl et al*. [2006] pointed out, the identification and computation of statistical metrics describing river morphology will greatly enhance the potential to calibrate and validate numerical models.

The aim of the present research is to address some of the research gaps and possibilities described above by investigating the effect of lateral confinement and formative discharge on gravel bed river planform and the detailed three-dimensional topography of the river bed. A set of 27 experiments with the same longitudinal slope and uniform grain size were designed to answer the following research questions:

I. To what extent does bed morphology change in response to different formative discharges within the constraints of different fixed channel widths? This question is posed because it provides a first step toward understanding the impact of changes in flow from, for example, flow regulation or regular hydropeaking on the bed morphology of real river channels with a confined width.
II. Is the bed elevation frequency distribution a good predictor of channel planform morphology? This question is posed because it is a first step toward incorporating the three dimensions of bed morphology into methods for discriminating between rivers of different planform style, including characterizing their physical (habitat) structure and thus building on existing two-dimensional indices such as the braiding index.
III. Is the areal extent of dry areas within the channel and its active width (i.e., the width over which sediment transport occurs) related to channel configuration, and can it be predicted from external controlling parameters? This question is posed because dry areas within the channel are indicative of islands in real rivers and thus the development of terrestrial or semiterrestrial areas, which are important for vegetation colonization and the biocomplexity of river ecosystems.

2. Methods

Twenty-seven experiments (Table 1) were carried out in a large flume (25 m long, 2.9 m wide) located at the University of Trento, Italy. The flume had a fixed longitudinal gradient (S) of 0.01 and was filled with well-sorted sand with a median grain size (d_s) of 1 mm (the sorting coefficient, computed as the square root of d_{84}/d_{16}, was 1.08). Each experiment was conducted within a fixed width channel, which varied among the experiments from 0.15 to 1.5 m. The nine different channel widths were achieved by lining the banks of a channel of the required width with a plastic sheet and then filling the channel with the sand bed material. Three fixed discharges (Q) were tested: 1.5, 2.0 and 2.5 L/s. During each experiment, sand was fed into the upstream part of the channel from a volumetric sand feeder at a constant rate equal to the average sediment flux exiting the flume (as determined in a preliminary phase of the run). At the downstream end of the flume, a chute conveyed the solid and liquid flux to a submerged tank where the sediment transport (Q_s) was measured by sampling the cumulative weight every minute.

The experiments reproduced hydraulic and morphological conditions that are common in gravel bed rivers and did not represent a model of a specific field prototype. Conditions were selected in order to ensure

Table 1. Summary Data of the Experimental Runs

Run #	W (m)	Q (L/s)	Wetted Width (m)	Dry Width (m)	Active Width (m)	Q_s (g/s)	Braiding Index	Active Braiding Index
1	0.15	1.5	0.15	0	0.15	3.55	1	1
2	0.15	2	0.15	0	0.15	6.88	1	1
3	0.15	2.5	0.15	0	0.15	7.52	1	1
4	0.2	1.5	0.2	0	0.2	3.54	1	1
5	0.2	2	0.2	0	0.2	5.15	1	1
6	0.2	2.5	0.2	0	0.2	7.10	1	1
7	0.3	1.5	0.3	0	0.3	3.06	1	1
8	0.3	2	0.3	0	0.3	4.56	1	1
9	0.3	2.5	0.3	0	0.27	6.64	1	1
10	0.4	1.5	0.4	0	0.32	1.87	1	1
11	0.4	2	0.4	0	0.36	3.57	1	1
12	0.4	2.5	0.4	0	0.36	5.41	1	1
13	0.6	1.5	0.57	0.03	0.33	1.57	1.25	1.10
14	0.6	2	0.59	0.01	0.41	2.99	1.13	1
15	0.6	2.5	0.59	0.01	0.42	5.09	1.10	1
16	0.8	1.5	0.73	0.07	0.33	1.79	1.76	
17	0.8	2	0.74	0.07	0.46	2.98	1.65	1.25
18	0.8	2.5	0.75	0.05	0.56	5.39	1.25	
19	1	1.5	0.87	0.13	0.35	1.15	1.81	1.40
20	1	2	0.90	0.10	0.39	2.05	1.50	1.14
21	1	2.5	0.91	0.10	0.48	3.30	1.55	1.30
22	1.25	1.5	0.96	0.29	0.39	1.01	2.53	1.64
23	1.25	2	1.02	0.23	0.45	1.71	2.20	1.50
24	1.25	2.5	1.04	0.21	0.53	2.97	1.88	1.43
25	1.5	1.5	1.07	0.44	0.30	1.02	2.47	1.54
26	1.5	2	1.15	0.35	0.41	2.18	1.81	1.57
27	1.5	2.5	1.22	0.29	0.50	2.86	2.15	1.62

turbulent flow in the areas where sediment transport occurred (Reynolds number $>$ 4000), and bed load transport dominated (cross-sectional average Shields stress ranging from 0.04 to 0.18). The depth over grain size ratio ranged from 7 to 30, as is typical of gravel bed rivers.

The duration of the experimental runs was set with reference to the conservation of sediment mass equation (the Exner equation), in order to reproduce a similar time scale for morphological evolution of the channel bed across different conditions. This time scale, T, can be expressed as

$$T = \frac{DW^2}{Q_s},$$

where D is average flow depth and W is channel width. Thus, T can be interpreted as the time needed for a bed change of the order of one depth on a longitudinal spatial scale of one channel width. A similar parameter was used by *Fujita* [1989] to quantify the evolution time scale of gravel bars. At a constant discharge, bed morphology is expected to reach a dynamic equilibrium in a few increments of T. This time scale ranged from about 5 to 650 min as a result of the 1 order of magnitude increase in channel width across the 27 experiments. Each experiment was run for a time period of approximately 10T to ensure a dynamic equilibrium between sediment transport, sediment output from the channel, and the bed morphology, and to enable collection of the data required for processing following completion of the experiments.

In each experiment, the mean sediment transport rate (Q_s) was calculated from sediment transport measurements once a dynamic equilibrium in sediment transport had been achieved. Toward the end of each experimental run, the morphology of the channel was recorded, including the dry areas that were not under water, wetted areas where sediment transport was occurring, the total number of channel branches, and the number of branches actively transporting sediment. The last two were recorded in order to compute the total and active braiding index, i.e., braiding indices calculated using all wetted channels and only those channels transporting sediment, respectively. These observations were performed manually on a set of 20 cross sections spaced at 0.5 m intervals within the central part of the flume and, in cases where the bed morphology was complex, measurements were obtained 2 or 3 times and then averaged. The spatial average of the braiding indices and of the different widths are reported in Table 1. In addition, a

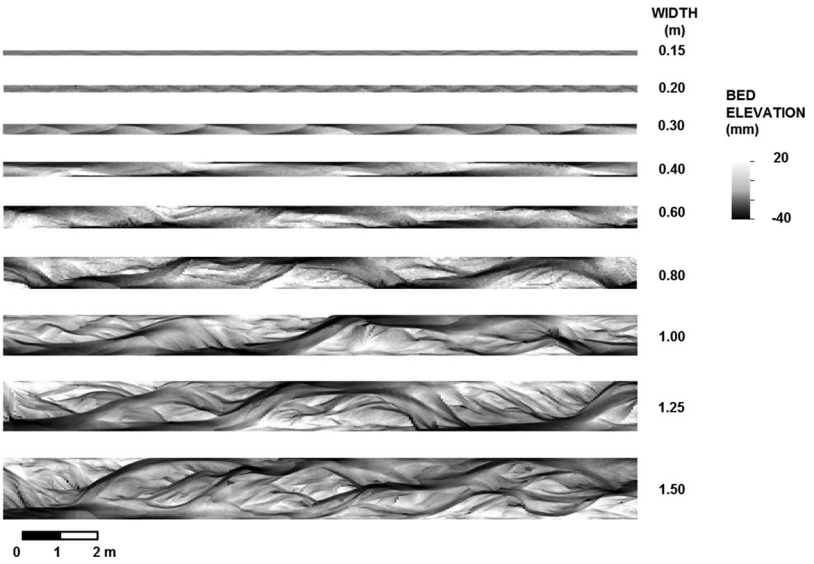

Figure 1. Set of detrended DEMs for the runs with a discharge equal to 2 L/s.

photographic survey was undertaken during each run, when the channel was under the full experimental discharge ("high flow"), using a Nikon D3100 SLR digital camera mounted on a hand-moveable carriage approximately 4 m above and parallel to the flume bed. A set of 16 pictures covered the entire flume. Dry areas were mapped on the stitched pictures to provide a more detailed estimation of the planform configuration. Immediately after the cessation of each run, a second set of pictures were obtained to represent "low flow" (i.e., water was still present, mostly in scoured areas and deep channels) to better visualize bed forms.

Following each experimental run, a digital elevation model (DEM) of the bed topography was obtained using a laser profiler supported on a bridge that was mounted on a rail positioned on the concrete walls of the flume. Bed elevation was recorded at 5 mm intervals across the flume and at 5 cm intervals along the flume to give a total of 150 cross sections in each survey. These data provided a detailed digital elevation model (DEM) of the channel form between 5 and 20 m along the flume length and thus excluding areas subject to entrance and outflow effects. Detrended DEMs were then constructed by subtracting the average bed slope (e.g., Figure 1). The detrended DEMs were then analyzed to extract descriptive statistics from the bed elevation frequency distribution, specifically the mean, median, standard deviation, skewness and kurtosis.

3. Results

3.1. Planform Morphology

The experimental setup allowed the effect of changing channel lateral confinement on bed morphology to be observed (e.g., Figure 1). In the following, we use the term "wandering" to classify channels with a transitional morphology between single thread and braiding [*Church*, 1983, 2006; *Carson*, 1984; *Knighton and Nanson*, 1993]. These are characterized by values of the total braiding index larger than one, but channel division is not continuous and is less intense than in braiding rivers. Channels were classified as "braided" when the total braiding index was larger than 1.5 or the active braiding index was larger than 1. Cases with a total braiding index ranging between 1 and 1.5 were classified as "wandering."

The narrowest channels (0.15 m) were characterized by a plane-bed, a near-rectangular cross section and intense sediment transport. Increasing the width to 0.2 m (and then 0.3 and 0.4 m) resulted in the formation of regular sequences of migrating alternate bars with wavelengths of approximately 7–10 times the channel width, which migrated downstream with variable speed of the order of a few centimeters per minute. At a width of 0.4 m, wetted areas that were not actively transporting sediment appeared (Figure 2) and were

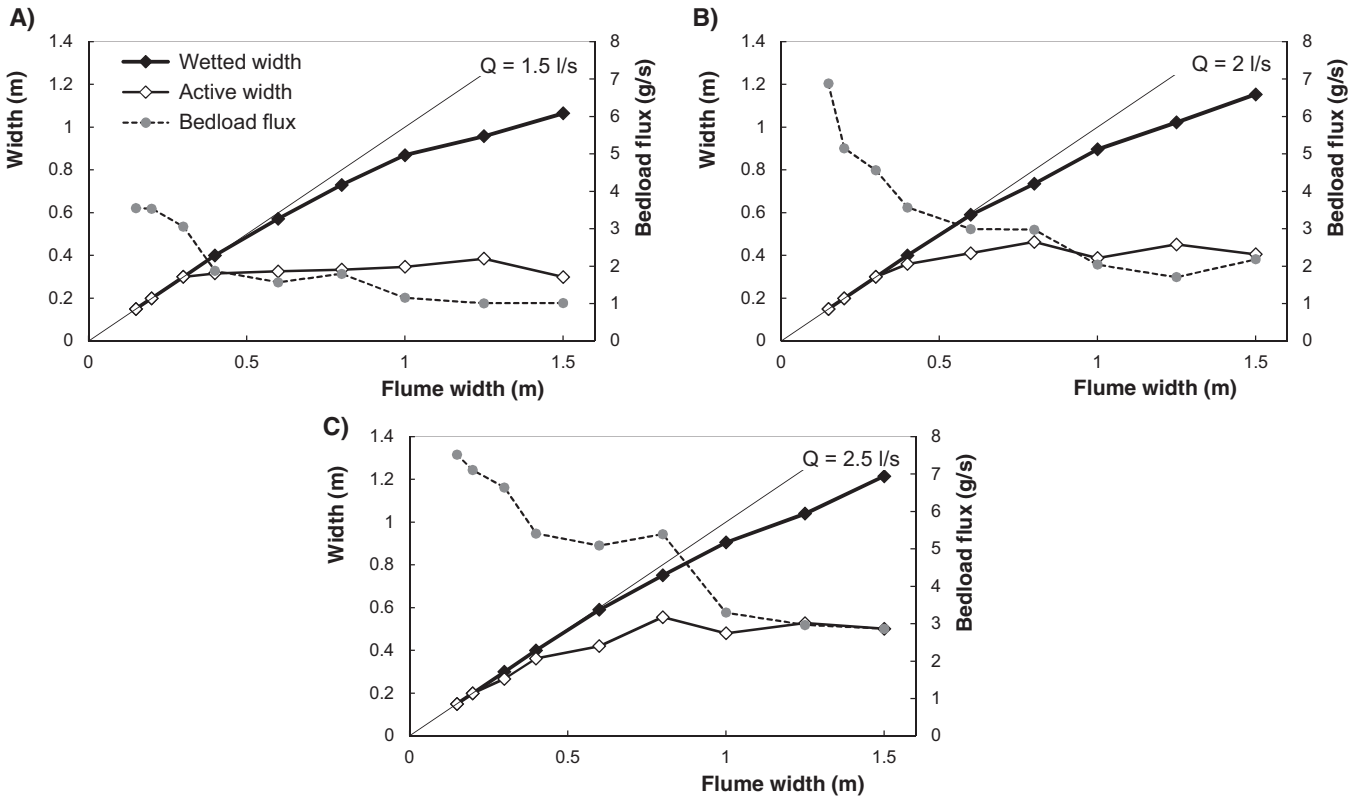

Figure 2. Changes in wet and active width, and in sediment flux, as a function of the flume width. Runs with (a) Q = 1.5 L/s; (b) Q = 2 L/s; and (c) Q = 2.5 L/s.

associated with a significant decrease in the average bed load flux. A further increase of the flume width to 0.6 m accentuated this behavior, causing the active width (i.e., the channel width within which sediment transport occurred) to fall below 70% of the total available width. This process had an effect on the channel morphology, slowing down bar migration and causing chute cutoffs. As a result, bed morphology was no longer characterized by regular sequences of alternate bars but showed a more complex configuration, resembling that of a wandering river. Dry areas started to appear on the tops of bars at a width of 0.8 m, further promoting the formation of lateral channels, and increasing the braiding index above an average value of 1.5. For discharges of 1.5 and 2 L/s, the configuration at this channel width is therefore defined as braided. Finally, with flume widths of 1, 1.25, and 1.5 m, the channel complexity continued to increase when quantified using both the total and the active braiding index. Interestingly, for the three largest widths, the active width remained almost constant for all three discharges, indicating that the combinations of gradient, flux, and grain size are able to maintain an active channel of approximately 0.35, 0.42, and 0.5 m, respectively. Similarly, the average sediment transport flux was almost constant, showing only a minor decrease with increasing flume width. The increased space available in these wider configurations was occupied in equal measure by dry areas and shallow channels not transporting sediments. In the case of the widest flume width (1.5 m), up to 30% of the channel was occupied by dry surfaces.

Four properties of the channel morphology produced by the experiments (dry width ratio, active width ratio, total braiding index, and active braiding index) are plotted with respect to dimensionless stream power in Figure 3. The dry and active width ratios are defined as the ratios between dry or active width, respectively, and the wetted width, whereas dimensionless stream power (ω) is defined as

$$\omega = \frac{QS}{W_w \sqrt{g \frac{\rho_s}{\rho_s - \rho_w} d_s^3}},$$

where W_w is the wetted width, g is gravitational acceleration, ρ_s is the measured sediment density, and ρ_w is the water density. This equation represents specific stream power normalized with the Einstein scale for

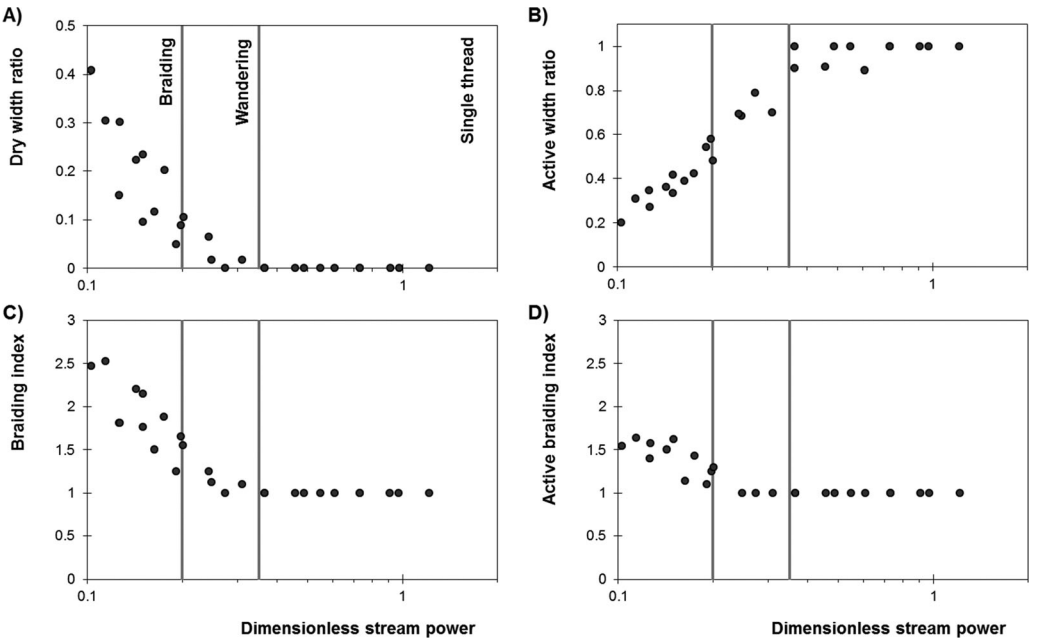

Figure 3. Relationship between (a) dry width ratio; (b) active width ratio; (c) braiding index; and (d) active braiding index; as a function of the dimensionless stream power.

sediment flux and has been found previously to describe the morphological configuration and bed load transport flux in braided networks effectively [see *Bertoldi et al*., 2009a]. The vertical lines in Figure 3 mark the transitions from a single thread to a wandering (ω larger than 0.37) and then to a braided configuration (ω less than 0.2). The dry width ratio increases for decreasing values of ω, with no dry areas (dry ratio equal to 0) for the single-thread configuration. Both braiding indices are equal to 1 and the active width ratio is larger than 0.9 for single-thread configurations, meaning that at least 90% of the cross section is actively involved in sediment transport. For values of dimensionless stream power lower than 0.37, all four parameters show an almost linear trend when dimensionless stream power is plotted on a logarithmic scale, highlighting a smooth transition from single-thread to fully braided configurations. These experiments show that a full range of planform configurations exists without any clear thresholds. In particular, the active width ratio shows an almost linear trend on the plot in Figure 3b, decreasing from 1 to 0.2 as values of dimensionless stream power decrease from 0.37 to 0.1. The active width ratio has been defined as a specific measure of braided rivers [*Ashmore et al*., 2011], but the present findings suggest it is relevant also for rivers with a transitional planform, where the active width of the channel ranges between 60% and 80% of the wetted width, despite the fact that the dry areas only account for about 5% of the area of the wetted surface. The active width ratio is quite difficult to measure in the field, and so the relationship between the dry width ratio (open symbols), the active width ratio (black symbols), and the braiding index observed in the experiments is plotted in Figure 4, as it may prove useful in estimating the proportion of field cross sections actively transporting sediment.

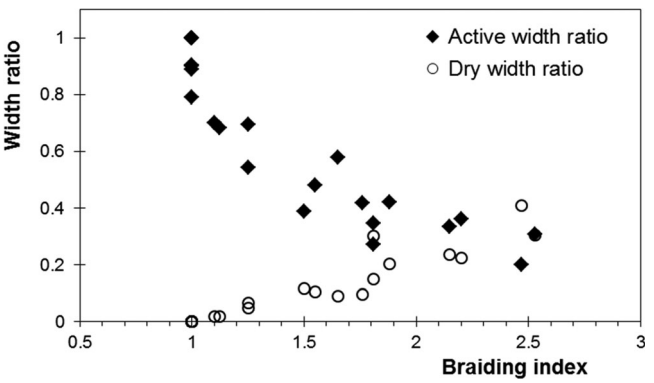

Figure 4. Active and dry width ratio as a function of the braiding index, for all experiments.

3.2. Sediment Transport Flux

The measured sediment transport flux, as evaluated from averaging over the equilibrium part of the runs (approximately 7–8 times the time scale T) is

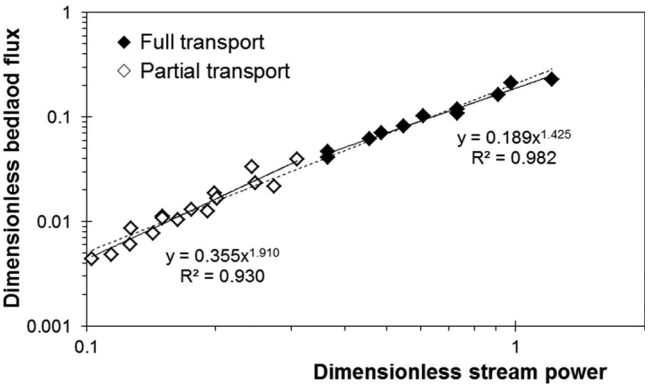

Figure 5. Normalized sediment transport flux as a function of the dimensionless stream power. Here we use the term "partial transport" to refer to cross sections with immobile areas.

plotted in Figure 5. Here the volume of sediment flux has been normalized in the same way as for stream power, by dividing it by the wetted width and by the Einstein scale to account for grain size. Figure 5 shows a clear relationship between dimensionless bed load flux and dimensionless stream power that is described by a power law (linear in a bilogarithmic plot). Experiments with fully transporting cross sections (active width ratio equal to 1) are plotted with closed symbols, whereas runs characterized by partially transporting cross sections are plotted with open symbols (here we use the term "partial transport" referring to cross sections with immobile areas, as in *Lisle et al*. [2000]). The two series are well approximated by a single statistically significant power relationship ($F = 1077$, degrees of freedom $= 1, 25$, $p < 0.001$) with an exponent of 1.61 ($t = 32.8$, $p < 0.001$) and an R^2 equal to 0.98. When estimated separately, the exponent changes from 1.43 for the fully transporting runs to 1.91 for the partially transporting runs. However, there is no statistically significant difference between these two exponents ($p > 0.05$), suggesting a uniform and steady increase in dimensionless sediment transport flux (per unit width) with stream power regardless of bed morphology.

3.3. Bed Topography

The availability of spatially detailed topographic data allowed the investigation of the effect of different levels of lateral confinement on the 3-D morphology of the channels. The 3-D morphology can be summarized in the form of an elevation frequency distribution (as reported in Figure 6 for each run) and such frequency distributions can be described quantitatively through descriptive statistics of the distribution's central tendency, dispersion, and shape. As the DEMs were detrended by expressing them as deviations from the average longitudinal slope and the experiments were designed to have a reach scale balance between the sediment input and output, the most commonly used descriptive statistic for central tendency, the mean elevation, was very close to 0 in all runs. In Figure 7, four further descriptive statistics of the bed elevation frequency distribution (the median, a measure of central tendency; the standard deviation, a measure of dispersion; the skewness and kurtosis, measures of shape in terms of distribution asymmetry and peakedness, respectively) are plotted against the log-transformed dimensionless stream power. In Figure 7, the same threshold values for the dimensionless stream power are shown as in Figure 3, separating single-thread, wandering, and braided configurations.

Strongly confined channels (W equal to 0.15 m, large values of ω) show a bed distribution characterized by a near Gaussian distribution with a median of approximately 0, very low values of the standard deviation, and skewness and kurtosis close to 0. This distribution is typical of a rectangular cross section, with small bed perturbations. Increasing the flume width to 0.4 m causes a rapid change in the bed elevation frequency distribution. The occurrence of alternate bars modifies the bed topography inducing an increase in the median value of the distribution to 3.5 mm, indicating that depositional areas are larger, but less vertically pronounced than scours. At the same time, the standard deviation increases up to about 10 mm, with skewness reaching values of -1.5 and kurtosis increasing to about 3. This last parameter shows a higher variability, due to its sensitivity to the occurrence of even a relatively small proportion of points with a very high or very low elevation (in particular scours deeper than 4 times the standard deviation). Planform configurations characterized by wandering or braiding patterns (values of the dimensionless stream power lower than 0.37) show less pronounced changes, with a slowly decreasing median (from 3.5 to 1 mm) and standard deviation (from 9 to 6 mm). Skewness and kurtosis are almost constant, showing negatively skewed distributions and positive values of kurtosis and thus indicating relatively peaked distributions but also with a high probability of extreme values (fatter tails).

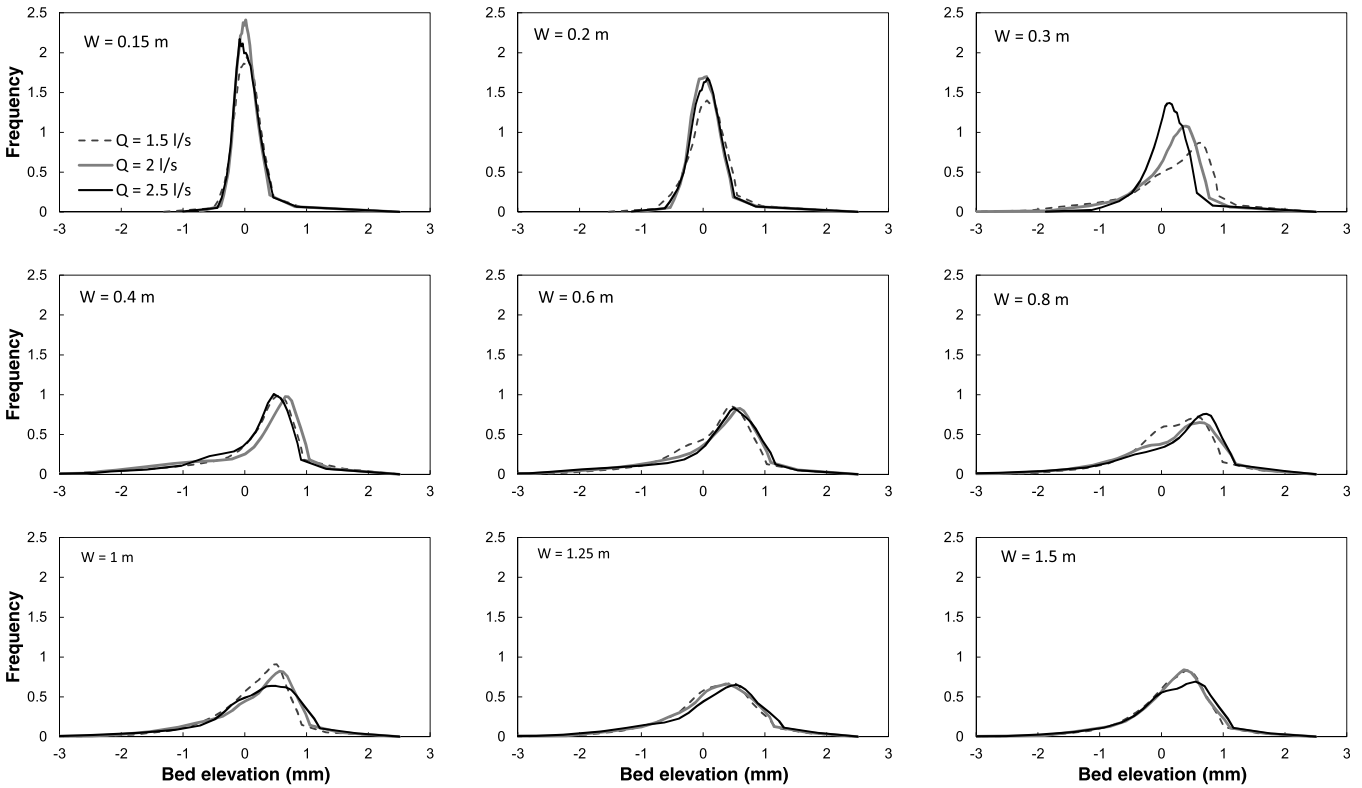

Figure 6. Bed elevation frequency distribution of the 27 runs. Each part corresponds to a different flume width.

Figure 8 shows the strong associations among the four parameters of the bed elevation frequency distribution and also the differences between single-thread, wandering, and braiding configurations. Figure 8a shows an almost linear relationship between median and standard deviation. Figure 8b shows linear relationships with two different slopes between skewness and kurtosis. No particular trend is evident that can help to differentiate the three planform styles. Very confined runs (flume width equal to 0.15 and 0.2 m) stand out from the rest, showing a quite different bed configuration, whereas all other points are located in the same area of the plots, with braiding showing slightly higher values of the standard deviation for the same value of the median and higher values of kurtosis for same value of skewness than the other planform styles.

4. Discussion

The research presented in this paper makes some valuable contributions to current knowledge of channel morphodynamics in three main areas: the active width or areal extent of particle movement as a function of channel morphological configuration and discharge; the association between channel planform style and summary statistics describing the three-dimensional topography of the river bed; the correspondence between our results and predictions for the formation of bars based on two analytical theories. Each of these areas is discussed below.

4.1. Active Width

Despite several published observations on the lateral variability of bed load transport in gravel bed rivers [e.g., *Gomez*, 1991; *Ferguson*, 2003; *Haschenburger and Wilcock*, 2003], to date little quantitative data have been produced that show the areal extent of particle movement as a function of formative discharge and morphological configuration, although the parameter "active width" has been introduced to investigate bed morphology versus sediment transport interaction in braided rivers [*Ashmore*, 2001; *Ashmore et al.*, 2011].

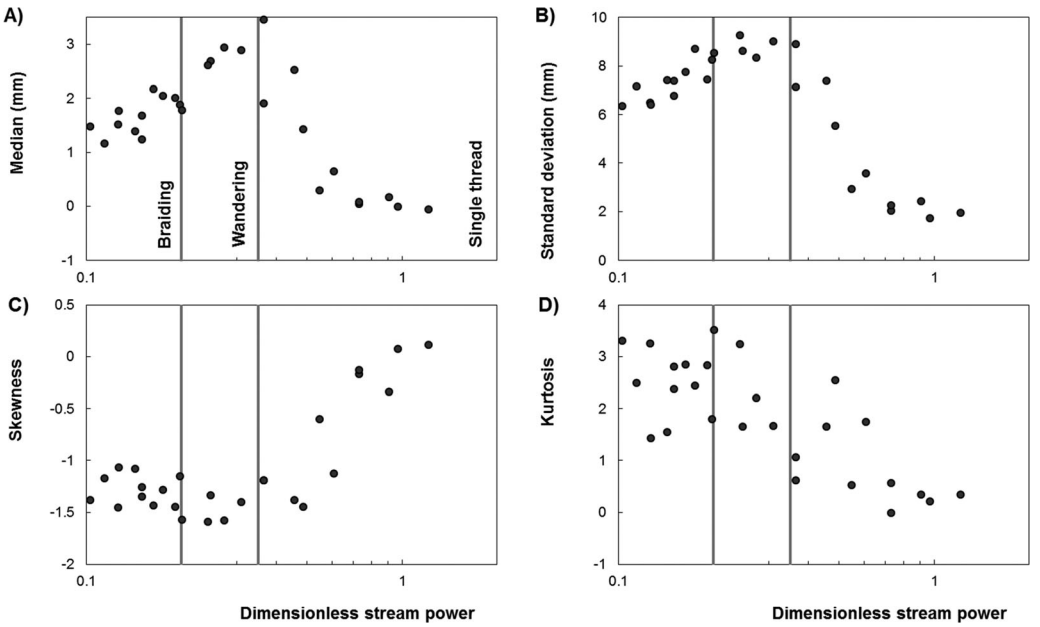

Figure 7. Bed elevation statistics as a function of the dimensionless stream power.

We compared previously published data on bed activity with our observations (Figure 9). Reported data have been elaborated in order to compute the same parameters we used (active width ratio and dimensionless stream power). This comparison shows similar trends and values, although in most of the previous analyses, active width was estimated from morphological changes, not from instantaneous observations of sediment transport as in the present case. In the case of multichannel networks, the proportion of the bed that is actively transporting sediment may be only a small fraction of the bed of wetted channels, even at formative discharge [*Bertoldi et al*., 2009b; *Ashmore et al*., 2011], whereas in single-thread rivers, *Lisle et al*. [2000] showed that between 10% and 80% of the bed area may have a negligible sediment transport flux. The data published by *Lisle et al*. [2000] follows a similar trend to that observed in the present experiments (Figure 3b), but with lower active width ratios. The discrepancy may be due to differences in grain size distribution and the occurrence of bed armoring. *Marti and Bezzola* [2006] performed a set of laboratory experiments on braided river sediment flux reporting that about 25% of the entire flume width was actively transporting sediments. From their published data, this should correspond to an active width ratio of 0.4,

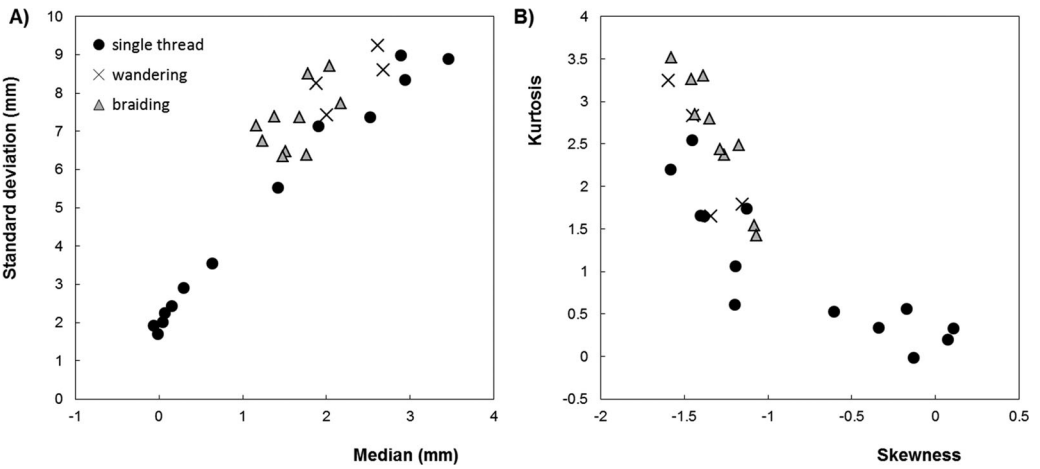

Figure 8. Relationships between the statistics of the bed frequency distribution.

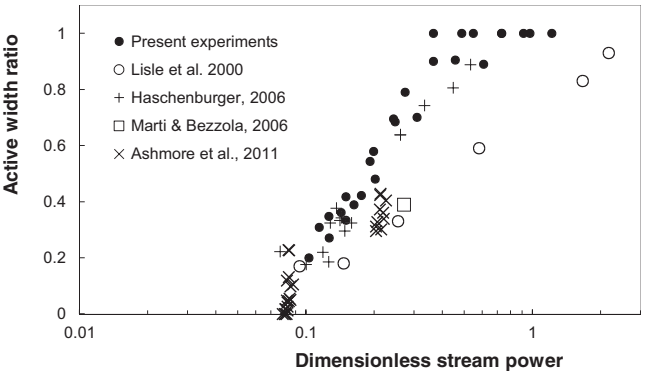

Figure 9. Active width ratio as a function of the dimensionless stream power for the present experiments and previously published field and laboratory data.

with a normalized unit stream power of 0.27. Also in their case, the active width is in a similar range to our data, with a slightly lower active ratio that can be explained by the grain size sorting. *Haschenburger* [2006] reports on measurements of scour and fill in the Carnation Creek (Canada) after 15 floods of different magnitude. She reported the proportion of points where no morphological changes were observed, which can be used to estimate an active width ratio. The data cover approximately the same range of dimensionless stream power as our runs and show a very close correspondence with our observations. It is worth noticing that in this case data do not refer to formative conditions, but to floods of different magnitude on the same reach.

The results presented in this paper confirm and extend those reported only for braided rivers by *Bertoldi et al*. [2009a] and *Ashmore et al*. [2011], and they also cover a much wider range of stream power. They, therefore, cross the spectrum from braided through wandering to single-thread channels, providing an integrated view across planforms and showing that there is a gradual transition from fully transporting cross sections to the complexity of braiding across this spectrum of planform types.

4.2. Bed Topography

The availability of high-resolution DEMs obtained from new survey techniques employing terrestrial laser scanners, airborne lidar, and structure-from-motion integration of photographs opens the possibility of developing new indicators that describe river bed topography in a more accurate way [*Brasington et al*., 2000; *McKean et al*., 2009; *Carbonneau et al*., 2012]. Bed elevation frequency distributions have the advantage of not being stage dependent (as, for example, is the braiding index). Results presented in Figures 6, 7, and 8 show that the bed elevation frequency distributions of river channels with different lateral confinement are different, particularly when comparing narrow (and simplified) bed morphologies, with more complex configurations. Our analysis also reveals that regular, alternate bars are the bed morphology with the highest bed elevation variability (highest values of the standard deviation). However, if the median and standard deviation are normalized with the average flow depth, the trend with dimensionless stream power (and thus planform style) changes (Figure 10). In this case, the median elevation scaled with flow depth increases rapidly from very narrow channels (high values of stream power in Figure 10a) with a median value around 0 to a value of around 0.25 for all the runs characterized by a wandering and a braided configuration. The effect of this scaling process is even more evident in relation to the standard deviation (Figure 10b), which shows continuously increasing values for decreasing values of the stream power across the three types of bed configuration. This illustrates that braided channels have the largest bed elevation variability, if it is scaled using the flow depth.

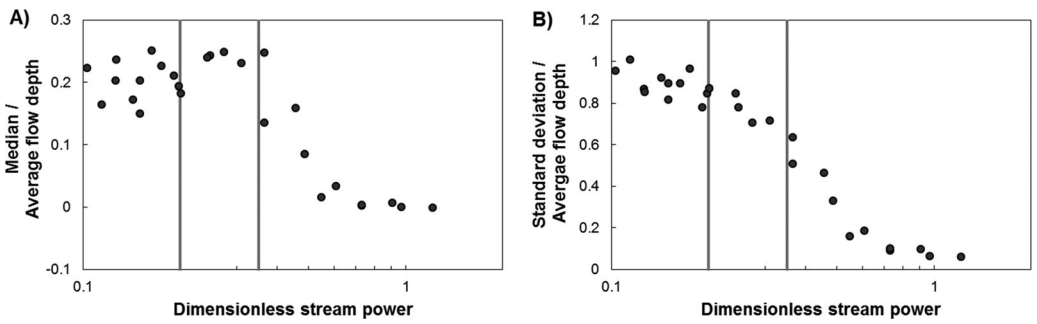

Figure 10. Median and standard deviation of the bed elevation frequency distribution normalized with the average flow depth.

These observations may be relevant when designing river restoration schemes, as different degrees of lateral confinement may result in different degrees of spatial variability of the bed topography and hence of the physical habitats that the bed presents. In addition, *Bertoldi et al*. [2011] showed that the colonization of riparian vegetation has a large impact on bed skewness, with more asymmetrical distributions (negative skewness) typical of unvegetated reaches, and more symmetrical bed configurations (skewness approximately 0) in the presence of vegetated bars and islands. Therefore, the quantification of the four parameters describing the bed frequency distribution may help to identify the morphological style of different river reaches and their deviation from the natural configuration.

In addition, these experiments may provide a good source of benchmark data to calibrate and validate numerical computational models, contributing to the definition of statistical metrics which also include topographic data [*Doeschl et al*., 2006]. 2-D depth averaged models are becoming more convincing [*Nicholas et al*., 2013], though correct reproduction of bank erosion is still challenging [*Jang and Shimizu*, 2005]. The possibility to test model results in different morphological conditions (ranging from straight, plane-bed channels to braiding channels), but with controlled, similar conditions in terms of slope, discharge, and grain size, may greatly help understanding of the potential and limits of these models.

4.3. Planform Style

In the last decade, considerable advances have been made in classifying channels based on both empirical relationships and physics-based theoretical analyses of bar development (two recent contributions are *Eaton et al*. [2010] and *Kleinhans and van den Berg* [2011]). The empirical approach generally considers the effect of external parameters (discharge, valley slope, and grain size) on natural river pattern and cannot take into account artificial constraints on the width (e.g., fixed embankments). With a different approach, the experiments reported here investigate changes in the river planform style (from straight to wandering to braiding) as determined by different degrees of lateral confinement. For this reason, we compare our results with the predictions of two analytical theories for the formation of bars, namely the free bar theory of *Colombini et al*. [1987] and the steady bar theory proposed by *Crosato and Mosselman* [2009]. Given a set of values for discharge, longitudinal slope, grain size, and channel width, both theories predict whether bars form and, if they do, their number (or bar mode) for each cross section. The free bar theory of *Colombini et al*. [1987] identifies a threshold value of the width to depth ratio, above which alternate bars form (mode 1). Larger channels (larger width/depth ratios) are needed to form central bars (mode 2) or multiple bars (mode 3 or more). *Crosato and Mosselman* [2009] provided an explicit equation to compute the most unstable bar mode:

$$m^2 = 0.17g \frac{(b-3)}{\sqrt{\frac{\rho_s}{\rho_s-\rho_w} d_s}} \frac{W_W{}^3 s}{CQ},$$

where C is the Chézy coefficient for roughness and b is a coefficient depending on the sediment transport equation, and then assuming a relationship between the bar mode (m) and the braiding index (B_i) of the form:

$$B_i = \frac{m-1}{2} + 1,$$

they directly evaluate the number of anabranches and the river planform style.

Table 2 compares the observed planform configuration from our experiments (single thread with plane-bed, single thread with alternate bars, wandering, and braiding), with the predicted bar type (alternate, central, or multiple) following *Colombini et al*. [1987] and the predicted planform style (meandering, transitional, and braiding) following *Crosato and Mosselman* [2009]. In the last case, two values of the parameter b have been tested. Crosato and Mosselman suggest that b = 5 should be used for sand bed rivers, and b = 10 for gravel bed rivers, in order to take account of the different sediment transport types (suspended versus bed load). Although the sediment used for our experiments is classified as sand, due to the scaling of the model, it actually represents a gravel bed, and sediments were transported only as bed load. Therefore, a value of b = 10 should better fit the experimental observations.

The results displayed in Table 2 show that both theories are reasonably good at predicting the transition from single thread to wandering and braiding. In particular, the theory of Crosato and Mosselman works

Table 2. Comparison Between Planform Style as Observed in the Experiments and Predicted by Free Bar Theory [*Colombini et al.*, 1987] and by Steady Bar Theory [*Crosato and Mosselman*, 2009], for Two Values of the Parameter b[a]

Run #	Observed Planform Style	Bar Type CST, 1987	Planform Style C&M, 2009 (b = 5)	Planform Style C&M, 2009 (b = 10)
1	Plane-bed	PLANE-BED	M	M
2	Plane-bed	PLANE-BED	M	M
3	Plane-bed	PLANE-BED	M	M
4	Alternate bar	PLANE-BED*	M	M
5	Alternate bar	PLANE-BED*	M	M
6	Alternate bar	PLANE-BED*	M	M
7	Alternate bar	ALTERNATE	M	T*
8	Alternate bar	ALTERNATE	M	M
9	Alternate bar	ALTERNATE	M	M
10	Alternate bar	ALTERNATE	M	T*
11	Alternate bar	ALTERNATE	M	T*
12	Alternate bar	ALTERNATE	M	T*
13	Wandering	MULTIPLE*	T	B*
14	Wandering	CENTRAL	T	B*
15	Alternate bar	CENTRAL*	T*	B*
16	Braided	MULTIPLE	B	B
17	Braided	MULTIPLE	B	B*
18	Wandering	MULTIPLE*	T	B*
19	Braided	MULTIPLE	B	B
20	Braided	MULTIPLE	B	B
21	Braided	MULTIPLE	B	B
22	Braided	MULTIPLE	B	B
23	Braided	MULTIPLE	B	B
24	Braided	MULTIPLE	B	B
25	Braided	MULTIPLE	B	B
26	Braided	MULTIPLE	B	B
27	Braided	MULTIPLE	B	B

[a]Asterisk (*) indicates wrong predictions. M is meandering, T is transitional, and B is braiding.

quite well when the parameter b is set to a value of 5, even if this should better represent the case of suspended sediments. With the suggested value of b = 10 to represent bed load transport, most of the runs close to the threshold between single thread and braiding are actually wrongly classified. Similarly, the linear theory of *Colombini et al.* [1987] predicts a larger number of bars (mode 2 or 3) in four cases (runs 13, 15, 17, and 18). This can probably be explained by the fact that both theories consider the case of small perturbations, neglecting the effect of thick bars (deposits of the order of the flow depth). Figure 11 shows a more detailed comparison of the observed braiding index and that predicted by Crosato and Mosselman. As also pointed out by *Kleinhans and van den Berg* [2011], this theory greatly overpredicts the braiding index. For example, when b = 10, the predicted braiding index is up to 3 times larger than that observed in the experiments.

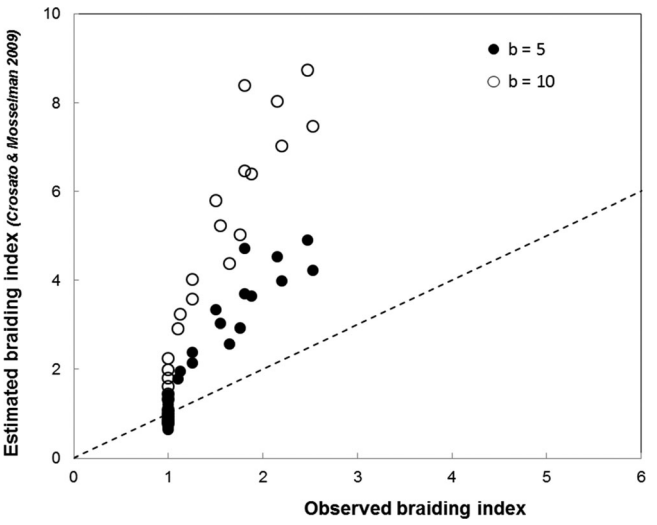

Figure 11. Comparison between observed and predicted [*Crosato and Mosselman*, 2009] braiding index. Two values of the parameter b are tested.

The observations of the active width reported in Figure 3b show that in the case of wandering and braiding configurations (dimensionless stream power lower than 0.37), sediments are transported only across a rather small fraction of the bed. This has important ecological implications, since it indicates that areas of stable bed coexist with areas where bed turnover and flushing occur. It is also important in a theoretical context, since all the analytical theories for bar formation are

based on the hypothesis that the entire width is actively transporting sediment. Their application in cases where the active width is smaller than the wetted width is, therefore, problematic. Direct observation of the bed morphology evolution during the experimental runs confirms that braiding is not a result of multiple bars forming in very wide and shallow channels but is more the result of a dynamic evolution of one or two main branches [*Ashmore*, 2001, 2013], where alternate or central bars form (because the active width is much lower than the full braid plain width) and then move laterally through bank erosion.

5. Conclusions

These laboratory experiments provide a first attempt to model the effect of changing channel width on bed morphology and planform style. They clearly show that there is a smooth transition between narrow, simple geometry channels and complex braided networks, which can be quantified using different morphological indices (e.g., braided index, exposed bed area, and parameters of the bed elevation frequency distribution), as well as through analysis of sediment transport processes.

The direct observation of the spatial and temporal patterns of bed load transport demonstrates that the occurrence of fully transporting cross sections is a relatively uncommon condition. Therefore, the active width ratio (previously introduced only to study braided rivers) has proved to be a relevant parameter to correctly assess sediment transport and morphological evolution of channels with bars and a wandering/transitional planform style.

This experimental approach shows that small changes in channel width can have significant impacts on bed form and spatial variability and thus on bed habitat complexity. In particular, we have shown that summary parameters of the bed elevation frequency distribution are much more effective at differentiating morphological complexity in single-thread channels than previously used indicators (e.g., braiding index and number of bars). These results have direct relevance to river restoration, since they indicate that even small increases in channel width can have beneficial effects for bed complexity and thus morphological quality. They are also relevant to the prediction of future river states, illustrating that any changes in river width or discharge impact on the form of the channel bed and the distribution and diversity of physical habitats that are present.

Nowadays, the increasing availability of accurate digital elevation models (extracted from lidar, terrestrial laser scanner, and structure-from-motion topographic surveys) makes the computation of bed elevation frequency distributions more easily achievable, opening new opportunities to better characterize river bed morphology. In future, the proposed approach and indicators would benefit from being tested and refined with real-world applications, under a wider range of flow and grain size conditions, providing information on the evolutionary trajectory of impacted rivers.

Acknowledgments
Alejandra Garcia Lugo's research is funded by the SMART Joint Doctoral Programme (Science for Management of Rivers and their Tidal systems), which is financed by the Erasmus Mundus Programme of the European Union. The authors thank Lorenzo Forti and Martino Salvaro for support in setting up and executing the experimental runs. Comments and suggestions by Jim Pizzuto, the Associate Editor, and an anonymous referee helped us improving the manuscript. Data of the flume experiments are available upon request to the corresponding author.

References

Ashmore, P. E. (2001), Braiding phenomena: Statics and kinetics, in *Gravel Bed Rivers V*, edited by M. P. Mosley, pp. 95–121, N. Z. Hydrol. Soc., Wellington.

Ashmore, P. E. (2013), Morphology and dynamics of braided rivers, in *Treatise on Geomorphology*, vol. 9, edited by J. Shroders and E. Wohl, pp. 289–312, Academic, San Diego, Calif.

Ashmore, P. E., W. Bertoldi, and T. J. Gardner (2011), Active width of gravel-bed braided rivers, *Earth Surf. Processes Landforms*, *36*, 1510–1521.

Bertoldi, W., P. E. Ashmore, and M. Tubino (2009a), A method for estimating the mean bed load flux in braided rivers, *Geomorpholgy*, *103*, 330–340.

Bertoldi, W., L. Zanoni, and M. Tubino (2009b), Planform dynamics of braided streams, *Earth Surf. Processes Landforms*, *34*(4), 547–557.

Bertoldi, W., A. M. Gurnell, and N. A. Drake (2011), The topographic signature of vegetation development along a braided river: Results of a combined analysis of airborne lidar, color air photographs, and ground measurements, *Water Resour. Res.*, *47*, W06525, doi:10.1029/2010WR010319.

Brasington, J., B. T. Rumsby, and R. A. McVey (2000), Monitoring and modelling morphological change in a braided gravel-bed river using high resolution GPS-based survey, *Earth Surf. Processes Landforms*, *25*(9), 973–990.

Carbonneau, P. E., M. A. Fonstad, W. Andrew Marcus, and S. J. Dugdale (2012), Making riverscapes real, *Geomorphology*, *137*(1), 74–86.

Carson, M. A. (1984), Observations on the meandering-braiding transition, Canterbury Plains, New Zealand. *N. Z. Geogr.*, *40*, 89–99.

Church, M. (1983), Pattern of instability in a wandering, gravel-bed channel, in *Modern and Ancient Fluvial Systems, Spec. Publ., 6*, edited by J. D. Collinson and J. Lewin, pp. 169–180, Int. Assoc. of Sedimentol, Blackwell, Oxford.

Church, M. (2006), Bed material transport and the morphology of alluvial river channels, *Annu. Rev. Earth Planet. Sci.*, *34*, 325–354.

Colombini, M., G. Seminara, and M. Tubino (1987), Finite amplitude alternate bars, *J. Fluid Mech.*, *181*, 213–232.

Crosato, A., and E. Mosselman (2009), Simple physics-based predictor for the number of river bars and the transition between meandering and braiding, *Water Resour. Res.*, *45*, W03424, doi:10.1029/2008WR007242.

Doeschl, A. B., P. E. Ashmore, and M. Davison (2006), Methods for assessing exploratory computational models of braided rivers, in *Braided Rivers: Process, Deposits, Ecology and Management, Spec. Publ. 36*, edited by G. H. Sambrook Smith et al., pp. 177–197, Blackwell, Oxford, U. K.

Eaton, B., R. G. Millar, and S. Davidson (2010), Channel patterns: Braided, anabranching, and single-thread, *Geomorphology*, *120*, 353–364.

Egozi, R., and P. E. Ashmore (2008), Defining and measuring braiding intensity, *Earth Surf. Processes Landforms*, *33*(14), 2121–2138.

Ferguson, R. I. (2003), The missing dimension: Effects of lateral variation on 1-D calculations of fluvial bedload transport, *Geomorphology*, *56*, 1–14.

Fotherby, L. M. (2009), Valley confinement as a factor of braided river pattern for the Platte River, *Geomorphology*, *103*, 562–576.

Fujita, Y. (1989), Bar and channel formation in braided streams, in *River Meandering, Water Resour. Monogr.*, vol. 12, edited by S. Ikeda and G. Parker, pp. 417–462, AGU, Washington, D. C.

Gomez, B. (1991), Bedload transport, *Earth Sci. Rev.*, *31*, 89–132.

Haschenburger, J. K. (2006), Observations of event-based streambed deformation in a gravel bed channel, *Water Resour. Res.*, *42*, W11412, doi:10.1029/2006WR004985.

Haschenburger, J. K., and P. R. Wilcock (2003), Partial transport in a natural gravel bed channel, *Water Resour. Res.*, *39*, 1020, doi:10.1029/2002WR001532.

Jähnig, S. C., S. Brunzel, S. Gacek, A. W. Lorenz, and D. Hering (2009), Effects of re-braiding measures on hydromorphology, floodplain vegetation, ground beetles and benthic invertebrates in mountain rivers, *J. Appl. Ecol.*, *46*, 406–416.

Jang, C. L., and Y. Shimizu (2005), Numerical simulation of relatively wide, shallow channels with erodible banks, *J. Hydraul. Eng.*, *131*, 565–575.

Kleinhans, M. G., and J. H. van den Berg (2011), River channel and bar patterns explained and predicted by an empirical and a physics-based method, *Earth Surf. Processes Landforms*, *36*, 721–738.

Knighton, A. D., and G. C. Nanson (1993), Anastomosis and the continuum of channel pattern, *Earth Surf. Processes Landforms*, *18*, 613–625.

Leopold, L. B., and M. G. Wolman (1957), *River Channel Patterns: Braided, Meandering, and Straight*, pp. 39–85, U.S. Gov. Print. Off., Washington, D. C.

Lisle, T. E., J. M. Nelson, J. Pitlick, M. A. Madej, and B. L. Barkett (2000), Variability of bed mobility in natural gravel-bed channels and adjustments to sediment load at local and reach scales, *Water Resour. Res.*, *36*, 3743–3755.

Marti, C., and G. R. Bezzola (2006), Bed load transport in gravel bed rivers, in *Braided Rivers: Process, Deposits, Ecology and Management, Spec. Publ., 36*, edited by G. H. Sambrook Smith et al., pp. 199–215, Blackwell, Oxford, U. K.

McArdell, B. W., and R. Faeh (2001), A computational investigation of river braiding, in *Gravel Bed Rivers V*, edited by M. P. Mosley, pp. 11–46, N. Z. Hydrol. Soc., Wellington.

McKean, J., D. Nagel, D. Tonina, P. Bailey, C. W. Wright, C. Bohn, and A. Nayegandhi (2009), Remote sensing of channels and riparian zones with a narrow-beam aquatic-terrestrial LIDAR, *Remote Sens.*, *1*, 1065–1096.

Nicholas, A. P., P. J. Ashworth, G. H. S. Smith, and S. D. Sandbach (2013), Numerical simulation of bar and island morphodynamics in anabranching megarivers, *J. Geophys. Res.*, *118*, 2019–2044, doi:10.1002/jgrf.20132.

Paola, C. (1996), Incoherent structures: Turbulence as a metaphor for stream braiding, in *Coherent Flow Structures in Open Channels*, edited by P. J. Ashworth et al., pp. 705–723, John Wiley, Chichester.

Parker, G. (1976), On the cause and characteristic scales of meandering and braiding in rivers, *J. Fluid Mech.*, *76*, 457–480.

Rohde, S., F. Kienast, and M. Bürgi (2004), Assessing the restoration success of river widenings: A landscape approach, *Environ. Manage.*, *34*(4), 574–589.

Rohde, S., M. Schütz, F. Kienast, and P. Engelmaier (2005), River widening: An approach to restoring riparian habitats and plant species, *River Res. Manage.*, *21*, 1075–1094.

Seminara, G., and L. Solari (1998), Finite amplitude bed deformations in totally and partially transporting wide channel bends, *Water Resour. Res.*, *34*(6), 1585–1598.

van den Berg, J. H. (1995), Prediction of alluvial channel pattern of perennial rivers, *Geomorphology*, *12*, 259–279.

van der Nat, D., A. P. Schmidt, K. Tockner, P. J. Edwards, and J. Ward (2002), Inundation dynamics in braided floodplains: Tagliamento River, northeast Italy, *Ecosystems*, *5*, 636–647.

Weber, C., E. V. A. Schager, and A. Peter (2009), Habitat diversity and fish assemblage structure in local river widenings: A case study on a Swiss river, *River Res. Appl.*, *701*, 687–701.

Welber, M., W. Bertoldi, and M. Tubino (2012), The response of braided planform configuration to flow variations, bed reworking and vegetation: The case of the Tagliamento River, Italy, *Earth Surf. Processes Landforms*, *37*, 572–582.